

Supplementary information

The Astonishing Progress in Performance of Hydrogel Triggered by the Structure Evolution of Cross-linking Junctions

Pengchong Li,^{a,b} Kun Xu,^{*a} Ying Tan,^a Cuige Lu,^{a,b} Yangling Li,^{a,b} Haiwei Wang,^{a,b} Xuechen Liang,^{a,b} and Pixin Wang^{*a}

^a Key Laboratory of Polymer Ecomaterials, Changchun Institute of Applied Chemistry, Chinese Academy of Sciences, Changchun, 130022, China.

E-mail: pxwang@caic.ac.cn; xukun@ciac.ac.cn

^b University of Chinese Academy of Sciences, Beijing, 100049, China.

1. Experiment Section

1.1 Materials

Acrylamide (AAm, Beihua Fine Chemical Co., Ltd) was twice recrystallized from acetone and vacuum dried at 40°C. Acrylate acid (AAc, Beihua Fine Chemical Co., Ltd) was purified by vacuum distillation. N-Vinylformamide (98%), tert-butylhydroperoxide (TBHP, 70% water solution), 2,2'-Azobis[2-(2-imidazolin-2-yl)propane] dihydrochloride (VA-044) and N,N'-methylenebisacrylamide (MBA) were used as received from Aldrich without further purification.

1.2 Synthesis of PVAm-graft-PAAcNa microgels

PVAm was prepared as following method. Poly (N-vinylformamide) (PNVF) was first synthesized by free radical polymerization in isopropyl alcohol using AIBN as initiator, followed by hydrolysis of PNVF in alkaline solution to obtain PVAm. The weight-average molecular weight of PVAm was 70,000 g mol⁻¹.

Microgels were prepared according to the previously reported literature.^[s1, s2] The typical synthetic procedure of microgels was as follows: Briefly, for a total aqueous solution of 30.00 g, purified AAc (1.20 g, 0.010 mol), and PVAm (0.30 g) were added sequentially into a three-necked flask equipped with a thermometer, a condenser, a magnetic stirrer and nitrogen inlet. The pH of the reaction solution was adjusted to 3-5 and the solid content was controlled at 5 wt%. After bubbling nitrogen for 30 minutes at 70°C, dilute TBHP solution (0.60 g, 0.1wt.% solution) was added to the mixture, and the solution was stirred at 70°C for 6 h under nitrogen for completing reaction. The final harvest mixture was a stable white translucent latex dispersion.

1.3 Synthesis of microgel composite hydrogels (MCH)

The synthetic procedure of MCH was described as follows: at first, a transparent aqueous solution consisting of appropriate mass of water and AAm (1.50 g) was prepared. Next, the aqueous solution including microgel nanoparticles and initiator (TBHP, 0.1wt% solution) were added to the former solution with drastic stirring at ice-

water bath. After the agents were completely mixed, the solution was transferred into test tubes of 15mm internal diameters and oxygen was excluded from the system. Free radical reaction was allowed to proceed in a water bath at 60 °C for 24 h to create the robust hydrogel with the shape of test tube. For comparison, the PAAm hydrogels with physically mixing microgels (MMH) were prepared by using initiator VA-044 instead of TBHP. During the preparation of the conventional organic cross-linking PAAm hydrogels (NMBA-H), NMBA was used as the cross-linker. Meanwhile, opaque MCH is soaked into alkali solution (pH=12) for a certain time interval until it becomes transparent and the time interval of alkali treatment depends on the size and shape of hydrogel. This transparent hydrogel after alkali treatment is denoted as T-MCH.

2. Characterization

2.1 Particle size analysis

The particle size and polydispersity index (PDI) of core-shell microgels were measured by dynamic light scattering using a Malvern Zetasizer 1000HSA (Malvern, Worcestershire, UK) at 25°C.

2.2 Super-resolution fluorescence microscopy (SRFM)

The SRFM is employed to investigate the structural evolution of microgel cross-linking junctions in composite hydrogel under the change of environmental pH. The as-synthesized MCH at pH=3 is first observed. And then the same sample is analysis again after it is soaked into alkali solution (pH=12) within several seconds until it becomes transparent. Finally, transparent MCH is treated in HCl solution (pH=3) within several seconds until it becomes opaque again. And it is investigated again with SRFM. The samples are 2mm thickness film and are fixed between slide glass and cover glass. The imaging experiment was performed on a Nikon Ti-E microscope. An objective-type total internal reflection fluorescence (TIRF) configuration using an oil-immersion objective (100×, NA 1.49, Nikon, Japan) was applied in the experiment. The fluorescence was filtered with emission filters and imaged on an EMCCD camera (Photometrics, Cascade II).

2.3 De-swelling dynamic

For the swelling experiment, the dried cylindrical samples with 3 mm diameter and 1 mm thickness were immersed into a large amount of DI water at room temperature with daily replacement of the water for one week to achieve the swelling equilibrium. Dynamic de-swelling behaviors of hydrogels were measured by recording weight of gels at fixed intervals when suddenly transferring equilibrated samples from DI water into acid solution (pH=3). The de-swelling rate of hydrogels were expressed as W_t/W_0 as a function of time, where W_t was the weight of hydrogels at t s and W_0 was weight at the beginning when the hydrogels were transferred into acid solution ($t_0=0$ s).

2.4 Turbidity measurements

The turbidity of the samples with 2mm thickness was measured at 500 nm by using UV-VIS spectrometer (Shimadzu UV-2401PC) under various pH condition at 25 °C.

2.5 ATR-FTIR analysis

The FT-IR spectra of hydrogel fragments were recorded on Thermo Nicolet Avetar 370 (Pike Technologies, Madison, WI) attenuated total reflection Fourier transform-infrared spectroscope (ATR-FTIR) in the range 4000–500 cm^{-1} .

2.6 Swelling ratio and swelling dynamic

For the swelling experiment, the dried cylindrical hydrogels with 3 mm diameter and 1 mm thickness were immersed into a large amount of DI water at room temperature with daily replacement of the water for one week to achieve the swelling equilibrium. The equilibrium swelling ratio was calculated from the ratio of the final wet weight of the swollen equilibrated gel (W_{gel}) to the weight of corresponding dried gel (W_{dry}). Dynamic swelling behaviors of hydrogels were measured by recording weight of gels at fixed intervals.

2.7 Compression measurements

The compressive stress-strain mechanical measurements were performed on various hydrogel samples with the same size (15 mm ϕ ×20 mm length) using an INSTRON-1121 tensile-compressive tester. The samples were measured at room temperature. Typically, the cylindrical gel sample was lubricated with dodecane to prevent drying and barreling, and then setted on the lower plate and compressed at a strain rate of 2 mm min^{-1} by the upper plate, which was connected to a load cell. The strength δ was calculated by $\delta = \text{Load}/\pi r^2$, where r was the initial unload radius. The strain ξ was defined as the change in the thickness relative to the free-standing thickness of specimen. The compressive modulus (E) was calculated from the slope at low strain (10%-20%).

2.8 Rheological measurements

Dynamic module were measured on the as-synthesized CH gels to evaluate the network chain density with a strain controlled rheology meter ARES-RFS (TA) using parallel plates of diameter 25mm. The cylindrical gel sample of the 25mm diameter and approximately 2mm thickness stuck the fixture well without slippage. First, the dynamic strain sweep was carried out at angular frequency of 1 rad/s to determine the linear viscoelasticity region. Then, frequency sweep was performed over the frequency range from 0.1 to 100 rad/s both in up and down directions at a constant shear strain 1%. All rheological measurements were carried out at $25 \pm 0.1^\circ\text{C}$ controlled by a Peltier plate.

3. Result and Discussion

3.1 The particle size and particle distributing index

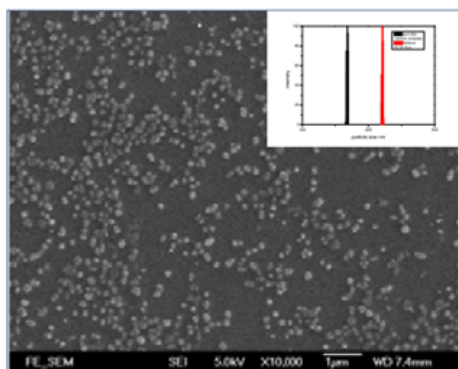


Figure S1. The SEM photograph of microgels and the little figure inserted shows the particle size and particle distributing index.

The SEM photograph and the result of DLS of microgels (Figure S1) show that the particle size and particle distributing index (PDI) are 240 nm and 0.045, respectively.

3.2 The pH-responsiveness of microgels

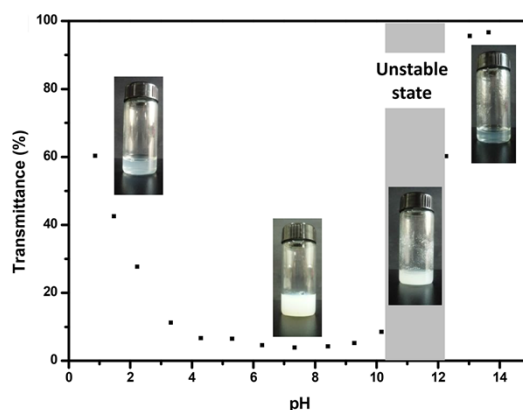


Figure S2. The transmittance of microgel dispersion vs. pH; the photographs inserted show that the appearance of microgel dispersions under various pH.

The microgels cross-linking junctions own obvious pH-responsiveness in that they are prepared via static-electrolyte complexation of grafting polyampholyte. From Figure S2, at pH=3 to 10, the microgel dispersion is white and opaque, whereas it becomes transparent at pH>12 owing to strong hydration stemming from complete ionization of carboxyl groups. At the same time, we can see that there is a unstable region of microgel dispersion at 10>pH>12, where large amount of precipitations occur. It should be attributed to stronger static-electrolyte interaction between carboxyl groups and amine groups in this designated pH region^[s3].

3.3 The de-swelling dynamic of various hydrogels

Table S1. The character parameters of various hydrogels shrinking process

Sample	Maximum SR ^[a] (%)	Shrinking time ^[b]			τ min
		SR=50%	SR=75%	SR=90%	
NMBA-H	63.80	350	- ^[c]	-	$\tau_1=4.38$ $\tau_2=413.22$
T-MCH	98.80	0.65	2	5	$\tau_1=2.76$ $\tau_2=25.95$
NMBA-H (NaCl)	3.50	- ^[d]	-	-	- -
T-MCH (NaCl)	95.20	105	240	420	$\tau_1=22.78$ $\tau_2=144.51$

^[a] SR is the abbreviation of shrinking ratio. ^[b] Herein, the shrinking time refers to the interval of time between starting point of hydrogel shrinking process and time points of 50, 75 and 90% shrinking ratio. ^[c] The maximum shrinking ratio of NMBA-H in aqueous solution is only 63.8%, and the corresponding time is ca. 2100 min. ^[d] The maximum shrinking ratio of NMBA-H in 0.15 M NaCl solution is 3.50%, which should be regard as keeping constant.

As for stimuli-responsive hydrogels, Tanaka et al.^[s4] have investigated the swelling-shrinking kinetic of hydrogels and pointed that the characteristic time (τ) for a hydrogels to swell or shrink is given by

$$\tau = \frac{l^2}{\pi^2 D}$$

Where l denotes the characteristic linear dimension of hydrogel and D is the collective diffusion coefficient of the networks. For a hydrogel, τ is related to the swelling ratio (M_t) and time (t) by

$$M_t \approx \frac{6}{\pi^2} \exp\left(-\frac{t}{\tau}\right)$$

The investigation of Ogawa et al.^[s5] has suggested that there is a good linear relation in the time course of the natural logarithm of the swelling degree (D_s) given by equation 2 in manuscript. In Fig. 3, it was observed that the plots for the deswelling of hydrogels rapidly increased at the initial stage, then increased gradually and reached an equilibrium value at last. Thus, approximate curves based on the deswelling kinetic were estimated by three stages^[s6] and two characteristic time.

In this paper, our aim is to illuminate the influence of structural evolution of cross-linking points on the structure and performance of MCH. As for as hydrogel materials is concentrated, their responsive characters, especially response rate, is crucial to the application of hydrogel. Thus, the response rate of de-swelling of various hydrogels is selected as prime research target of our work.

3.4 The mechanical performance of various hydrogels

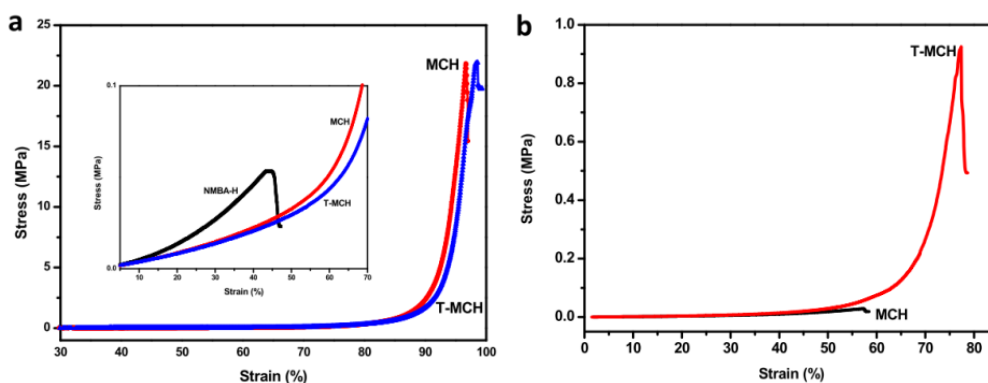


Figure S3. The compressive strength of samples. a. as-prepared hydrogels with 82.5 wt% water; b. hydrogels containing 98.0 wt% water.

In this paper, the evolution of microgel cross-linking junction can also lead to the development of mechanical performance of MCH. Compared with compressive strength of as-prepared MCH and T-MCH, they both remain intact bearing tremendous pressure (more than 20 MPa) and no obvious difference can be found owing to their lower water content. However, when water content increases and is controlled at 98.0%, significant difference occurs. As shown in Figure S3, the compressive strength of T-MCH can be up to 0.925 MPa, whereas that of MCH is only 0.028 MPa.

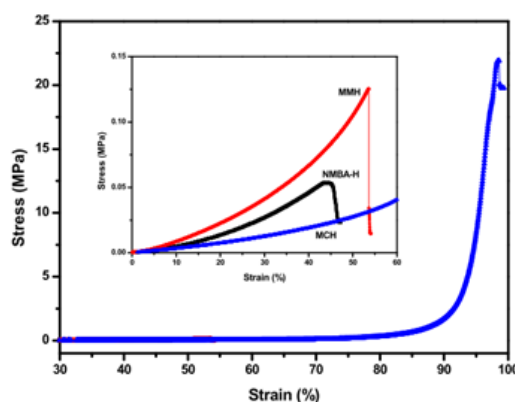


Figure S4. The stress-strain curves of MMH, NMBA-H and MCH.

MCH can remain intact under tremendous pressure and the compressive strength can be more than 20 Mpa because of the energy dissipation mechanism of microgel cross-linking junctions. As a comparison, organic cross-linking hydrogel and microgel mixing hydrogel are also synthesized and are denoted as NMBA-H and MMH, respectively. Unfortunately, the compressive strength of NMBA-H and MMH are only 0.06 and 0.13 Mpa, respectively (Figure S4).

3.5 The FTIR analysis of PAAm hydrogel matrix

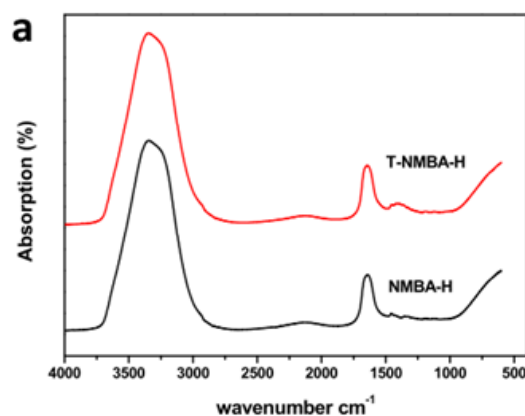


Figure S5: the ATR-FTIR of NMBA-H and alkali-treated NMBA-H.

In this section, the structure of NMBA-H and T-NMBA-H are analyzed by FTIR to illuminate the structural change of them. As shown in Figure S5, the structural change of NMBA-H is undetectable and this result suggests that the hydrolysis degree of PAAm chains in cross-linking network is negligible.^[s7]

3.6 The swelling dynamic of MCH and T-MCH

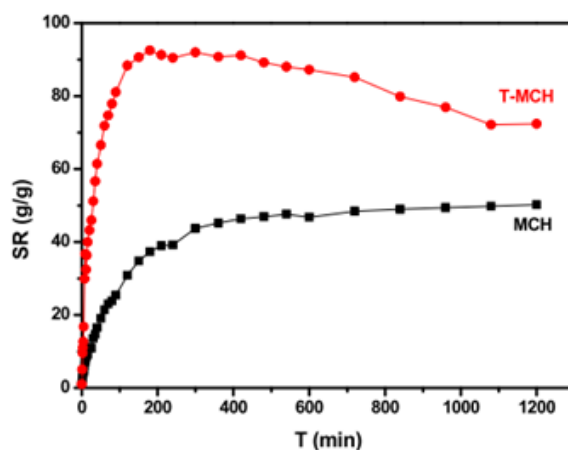


Figure S6: the swelling dynamic curves of MCH and T-MCH in distilled water.

In the case of a hydrogel swelling behaviors from a dry state, the swelling rate is far slower than that of deswelling rate, and no difference in swelling rate can be found between MCH and T-MCH. However, the swelling processes of them are totally different (as shown in Figure S6). The swelling ratio of MCH increases in proportion to the square root of time, whereas the swelling ratio of T-MCH increases to a maximum and gradually shrinks to an equilibrium state. This special swelling behavior of T-MCH perhaps should be contributed to the static-electrolytic interaction between various charges of grafting copolymer chains in T-MCH network.^[s8]

References

- [s1] M. F. Leung, J. M. Zhu, F. W. Harris, and P. Li, *Macromol. Rapid. Commun.* 2004, 25, 1819-1822.
- [s2] P. Li, J. M. Zhu, P. Sunintaboon, and F. W. Harris, *Langmuir*. 2002, 18, 8641-8646.

- [s3] Q. Zhang, S. B. Zhang, S. H. Li, *Int. J. Hydrogen Energy*. 2011, 36, 5512-5520.
- [s4] T. Tanaka, E. Sato, Y. Hirokawa, S. Hirotsu, J. Peetermans, *Phys. Rev. Lett.* 1985, 22, 2455-2458.
- [s5] Y. Ogsawa, K. Ogawa, E. Kokufuta, *Langmuir*. 2004, 20, 2546-2552.
- [s6] M. Takekawa, E. Kokufuta, *Colloid. Polym. Sci.* 2009, 287,323-334.
- [s7] E. Mueller, A. Blume, *Biochim. Biophys. Acta.* 1993, 1146, 45-51.
- [s8] K. Xu, J. H. Wang, Q. Chen, Y. M. Yue, W. D. Zhang, and P. X. Wang, *J. Colloid. Interface. Sci.* 2008, 321, 272-278.